PHYSICAL REVIEW D **75,** 013003 (2007)

Neutrino phenomenology of very low-energy seesaw scenarios

André de Gouvêa, James Jenkins, and Nirmala Vasudevan

Northwestern University, Department of Physics & Astronomy, 2145 Sheridan Road, Evanston, Illinois 60208, USA

(Received 18 August 2006; published 9 January 2007)

The standard model augmented by the presence of gauge-singlet right-handed neutrinos proves to be an ideal scenario for accommodating nonzero neutrino masses. Among the new parameters of this ''new standard model'' are right-handed neutrino Majorana masses M. Theoretical prejudice points to M much larger than the electroweak symmetry breaking scale, but it has recently been emphasized that all M values are technically natural and should be explored. Indeed, M around 1–10 eV can accommodate an elegant oscillation solution to the liquid scintillator neutrino detector (LSND) anomaly, while other M values lead to several observable consequences. We consider the phenomenology of low-energy ($M \lesssim$ 1 keV) seesaw scenarios. By exploring such a framework with three right-handed neutrinos, we can consistently fit all oscillation data—including those from LSND—while partially addressing several astrophysical puzzles, including anomalous pulsar kicks, heavy element nucleosynthesis in supernovae, and the existence of warm dark matter. In order to accomplish all of this, we find that a nonstandard cosmological scenario is required. Finally, low-energy seesaws—regardless of their relation to the LSND anomaly—can also be tested by future tritium beta-decay experiments, neutrinoless double-beta decay searches, and other observables. We estimate the sensitivity of such probes to M.

DOI: 10.1103/PhysRevD.75.013003 PACS numbers: 14.60.St, 14.60.Lm, 14.60.Pq

I. INTRODUCTION

Neutrinos have provided our first glimpse into physics beyond the standard model of elementary particles (SM). Neutrino oscillation experiments have given us unambiguous evidence that the three active neutrinos have mass and mix (see [1] for recent reviews of neutrino theory and phenomenology). As most important discoveries, the results of these experiments have raised more questions than they answered. Even from our limited knowledge of the neutrinos, it is clear that their properties, including sub-eV masses and large mixing, are quite different from their charged fermion counterparts. The true explanation of this puzzling behavior likely rests on the fact that neutrinos are the only known fundamental neutral fermions, but the exact reason behind this is still open to speculation. Neutrino masses, as deduced from oscillation experiments, hint at the existence of right-handed neutrino states, lepton-number violation, new sources of CP violation, as well as a new energy scale.

The seesaw mechanism [2] is an appealing way to generate the observed neutrino masses and lepton mixing matrix. The idea is simple. Add an arbitrary number of singlet fermion states to the SM matter content. The triviality of their quantum numbers allows them to have Majorana masses of magnitude M, as well as couple to the $SU(2)_L$ lepton and Higgs doublets. The latter vertices become Dirac mass terms of magnitude μ after electroweak symmetry breaking. The standard theoretical prejudice is that the Dirac masses are of order the charged fermion masses, while the Majorana masses are at some very high-energy scale, $M \gg 100$ GeV. If this is indeed the case, the resulting propagating neutrino degrees of freedom separate into two quasidecoupled groups: mostly active states with very small masses $m \sim \mu^2/M$ suppressed by the new physics scale and mostly sterile states with very large masses M. In this scenario, the mostly right-handed states are not directly observable. Indeed, it is possible that if such a high-energy seesaw is realized in nature, its only observable consequence is that the mostly active neutrinos have mass and mix.

Of course, there is no direct evidence that M—which we refer to as the seesaw scale— is large. Large M values are attractive for several reasons, including the fact that one may relate M to the grand unified scale. On the other hand, all M values are technically natural, given that when M vanishes the global symmetry structure of the Lagrangian is enhanced: $U(1)_{B-L}$ is a symmetry of the Lagrangian if $M = 0$, so that M is often referred to as the lepton-number breaking scale. This point was recently emphasized in [3]. Recent analyses have also revealed that there are several low-energy choices for the seesaw energy scale that allow one to address outstanding problems in particle physics and astrophysics. The main reason for this is that, unlike in the high-energy seesaw, in a low-energy seesaw the mostly right-handed states do not decouple but remain as kinematically accessible sterile neutrinos.

The data reported by the LSND short-baseline neutrino oscillation experiment [4] can be explained by postulating the existence of light ($m \sim$ 1–10 eV) sterile neutrino states. This result is currently being tested by the Fermilab MiniBooNE experiment [5] and, if confirmed, will lead the community to seriously contemplate the existence of light, SM singlet fermions. It was pointed out in [3] (see also [6]) that if $M \sim$ 1–10 eV, the right-handed seesaw neutrinos can easily play the role of the LSND sterile neutrinos. There is also evidence for mixed sterile neutrinos at other energy scales: eV sterile neutrinos aid in

heavy element nucleosynthesis in supernovae, keV sterile neutrinos can help explain the peculiar velocity of pulsars, and remain viable warm dark matter candidates. In the past several months, it has been shown that the seesaw right-handed neutrinos may play the role of all these astrophysically/cosmologically inspired sterile neutrinos [7,8].

In this paper, we consider the phenomenology of low-energy ($M \lesssim 1$ keV) seesaw scenarios, extending the analysis performed in [3] in several ways. In Sec. II, we review the generation of neutrino mass via the seesaw mechanism and apply it to relatively light right-handed neutrino states. We pay special attention to the most general active-sterile seesaw mixing matrix, whose parameters are the main object of our study. In Sec. III, we review the several different ''evidences'' for sterile neutrinos and discuss whether these can be ''fit'' by the low-energy seesaw. We concentrate on exploring solutions that can accommodate at the same time the LSND anomaly and the astrophysical processes outlined above, but we also discuss different combinations of the seesaw parameters capable of explaining only the astrophysics-related observables. In Sec. IV, we examine other experimental probes that can be used to explore low-energy seesaws—regardless of their relationship to the LSND anomaly, pulsar kicks, and warm dark matter. We concentrate on the prospects of current/future tritium beta-decay and neutrinoless double-beta-decay experiments. We conclude in Sec. V by summarizing our results, commenting on the plausibility of this scenario, and offering a general outlook for the future.

II. THE SEESAW MECHANISM AND ELECTRON VOLT NEUTRINO MASSES: PRELIMINARIES

In order to account for nonzero neutrino masses, we add to the SM particle content three $SU(3)_c \times SU(2)_L \times U(1)_Y$ gauge-singlet fermion states N_i, conventionally referred to as right-handed neutrinos. While sterile under SM gauge interactions, right-handed neutrinos may still be charged under new, currently unknown gauge transformations. Such interactions, if at all present, are neglected in our analysis.

The most general renormalizable Lagrangian consistent with SM gauge invariance is

$$\mathcal{L}_\nu = \mathcal{L}_{\rm old} - \lambda_{\alpha i}\bar{L}^\alpha H N^i - \sum_{i=1}^{3}\frac{M_i}{2}\bar{N}^{ci}N^i + \text{H.c.}, \quad (2.1)$$

where $\mathcal{L}_{\rm old}$ is the traditional SM Lagrangian, H is the Higgs weak doublet, L^α, $\alpha = e, \mu, \tau$ are lepton weak doublets, $\lambda_{\alpha i}$ are neutrino Yukawa couplings, and M_i are Majorana masses for the N_i. We choose, without loss of generality, the Majorana mass matrix M_R to be diagonal and its eigenvalues M_i to be real and positive. We also choose the charged-lepton Yukawa interactions and the charged weak-current interactions diagonal so that all physical mixing elements are contained in the neutrino sector.

After electroweak symmetry breaking (when H develops a vacuum expectation value v), $\mathcal{L}_\nu$ will describe, aside from all other SM degrees of freedom, six neutral massive Weyl fermions—six neutrinos. The resulting mass terms can be expressed as

$$\mathcal{L}_\nu \supset \frac{1}{2}\begin{pmatrix}\vec{\nu} & \vec{N}^C\end{pmatrix}\begin{pmatrix}0 & \mu \\ \mu^T & M_R\end{pmatrix}\begin{pmatrix}\vec{\nu}^c \\ \vec{N}\end{pmatrix}, \quad (2.2)$$

where $\mu \equiv \lambda v$, and $\vec{\nu}$ and $\vec{N}$ are vectors of the three active neutrinos (ν_e, ν_μ, ν_τ) and the three right-handed, sterile states, respectively. Each entry in the symmetric mass matrix of Eq. (2.2) is itself a 3×3 matrix of mass parameters. Diagonalization of the mass matrix yields eigenstates with Majorana masses that mix the active-active states, related via the standard lepton mixing matrix V, and the active-sterile states. The physical neutrinos are thus linear combinations of all active and sterile states. Throughout we will work in the ''seesaw limit,'' defined by $\mu \ll M_R$. In this case, there are three mostly active light neutrinos and three mostly sterile heavy neutrinos where ''mostly'' is determined by the induced mixing parameters.

In the seesaw limit, the diagonalization is simple. Assuming, for simplicity, that the mixing matrices are real,

$$\begin{aligned}\begin{pmatrix}0 & \mu \\ \mu^T & M_R\end{pmatrix} &= \begin{pmatrix}1 & \Theta \\ -\Theta^T & 1\end{pmatrix}\begin{pmatrix}V & 0 \\ 0 & 1\end{pmatrix}\begin{pmatrix}m & 0 \\ 0 & M_R\end{pmatrix} \\ &\quad \times \begin{pmatrix}V^T & 0 \\ 0 & 1\end{pmatrix}\begin{pmatrix}1 & -\Theta \\ \Theta^T & 1\end{pmatrix} + \mathcal{O}(\Theta^2),\end{aligned} \quad (2.3)$$

where m is the diagonal matrix of light neutrino masses and Θ is a matrix of active-sterile mixing angles found from the relations

$$\Theta M_R = \mu, \quad (2.4)$$

$$\Theta M_R \Theta^T = -VmV^T. \quad (2.5)$$

The elements of Θ are small [$\mathcal{O}(\mu/M_R)$], and the standard seesaw relation ($VmV^T = -\mu M_R^{-1}\mu^T$) is easily obtained by combining Eqs. (2.4) and (2.5). On the other hand, using Eq. (2.5), we can relate the mixing parameters in Θ to the active-active mixing angles contained in V and the neutrino mass eigenvalues. In the case of observably light sterile neutrino masses, as considered in our analysis, this equation is very useful, as it places testable constraints on observable quantities. The general solution (first discussed in detail in [9]) of Eq. (2.5) is

$$\Theta = -Vm^{1/2}OM_R^{-1/2}, \quad (2.6)$$

where O is an orthogonal matrix parameterized by three mixing angles ϕ_{12}, ϕ_{13}, ϕ_{23}.[1] Physically, the mixing ma-

[1]In general, O is a *complex* orthogonal matrix. Here, however, we will restrict our analysis to *real* neutrino mass matrices, unless otherwise noted.

trix O is a consequence of our freedom to choose the form of M_R. An illustrative example is found by considering the mass ordering of M_R in its diagonal form. The reordered matrix $M_R(m_i \leftrightarrow m_j)$ is equivalent to a $\pi/2$ rotation in the $i-j$ plane and therefore represents the same physics as the original matrix, as it should. In other words, OM_RO^T is the physically relevant object, as opposed to O and M_R separately. This object, when constrained to be real, has six free parameters that we shall refer to as "heavy parameters": ϕ_{12}, ϕ_{13}, ϕ_{23}, M_1, M_2, M_3.

Using Eq. (2.6), the 6×6 unitary neutrino mixing matrix is

$$U = \begin{pmatrix} V & \Theta \\ -\Theta^T V & 1 \end{pmatrix}. \tag{2.7}$$

Note that, up to $\mathcal{O}(\Theta^2)$ corrections, V is unitary. U is entirely described in terms of the three light mixing angles, six mass eigenvalues and three angles ϕ_{ij}. Many combinations of these have been measured or constrained via oscillation searches, cosmology and astrophysics. In particular, the two active neutrino mass-squared differences and mixing angles have been measured [1,10,11], thus leaving free the six heavy parameters and the absolute scale of active neutrino masses.[2] With U, the corresponding neutrino mass values, and the SM couplings we can calculate all observable quantities and compare them with data.

It is natural to wonder how well the seesaw approximation holds once one starts to deal with M_R values around 1 eV. From Eq. (2.4), it is clear that one can choose for the expansion parameter $\sqrt{m/M_R}$. In all scenarios considered here, $\sqrt{m/M_R} < 0.5$ (for $M \sim 1$ eV and $m \sim 0.3$ eV). In the worst case scenario, therefore, first order corrections are 55% of the leading order terms, while second order corrections are near 30%. Corrections to most observables of interest are much smaller than this because they are suppressed by larger right-handed neutrino masses. The first nontrivial correction to Eq. (2.6) occurs at second order and we find that, for the ambitions of this paper, all approximations are under control. This simple argument has been verified numerically for the most worrisome cases.

Before concluding this section, we wish to add that operators that lead, after electroweak symmetry breaking, to Majorana masses for the left-handed neutrino states (M_L) are also allowed if one introduces $SU(2)_L$ Higgs boson triplets or nonrenormalizable operators to the SM Lagrangian. While we neglect these "active" Majorana masses, we caution the reader that the existence of such terms would alter our results significantly. In particular, assuming the seesaw approximation holds, Eq. (2.5) would read

$$VmV^T + \Theta M_R \Theta^T = M_L, \tag{2.8}$$

which leads to a relationship between Θ, m, and M_R different from Eq. (2.6). If this were the case, for example, it would no longer be true that the largest Θ value (in absolute value) is constrained to be smaller than $(m_{\max}/M_{R,\min})^{1/2}$, where $m_{\max}$ is the largest element of m, while $M_{R,\min}$ is the smallest element of M_R. On the other hand, all objects on the left-hand side of Eq. (2.8) are observables. Hence, in the case of a low-energy seesaw, one can expect, in principle, to be able to test whether there are contributions to the neutrino mass matrix that are unrelated to the presence of right-handed neutrinos. By measuring V, m, M_R, and Θ, one can establish whether M_L is consistent with zero.

III. OSCILLATION PHENOMENOLOGY AND CURRENT EVIDENCE FOR LOW-ENERGY SEESAW

Here we examine a number of experimental and observational anomalies that may be explained by light sterile neutrinos. More specifically, we explore what these can teach us about the currently unknown parameters of the seesaw Lagrangian, described in detail in Sec. II. In all cases we assume three mostly active and three mostly sterile neutrinos and, most of the time, will concentrate on a $3+2+1$ picture of neutrino mass eigenstates, that is, three mostly active sub-eV neutrinos, two mostly sterile eV neutrinos, and one almost completely sterile keV neutrino. The hope is that the heavier state can account for warm dark matter (Sec. III B) or pulsar kicks (Sec. III C), which both require at least 1 keV neutrino, while the other two mostly sterile states help "explain" the existing oscillation data where, for all practical purposes, the heaviest neutrino decouples and we are left with an effective $3+1$ or $3+2$ picture. We remind readers that a third possibility ($2+2$[3]) is currently ruled out by solar and atmospheric data [12–14] and will be ignored. $3+1$ schemes that address the LSND anomaly are also disfavored by global analysis of short-baseline oscillation experiments [12–15] and, for this reason, we mostly concentrate on $3+2$ fits to the LSND anomaly [15].

Our analysis method is as follows: For each experimental probe considered we perform a χ^2 "fit" of the mixing matrix U, given by Eq. (2.7), and neutrino masses to the "data," and extract the region of parameter space that best explains the data. In most cases we allow the light mixing angles and mass-squared differences to vary within their 1σ limits (according to [10]),[4] the angles ϕ_i to vary uncon-

[2]The active neutrino mass hierarchy, normal vs inverted, is another (discrete) free parameter.

[3]It would have been rather difficult to construct a $2+2$ neutrino mass hierarchy using the seesaw Lagrangian.

[4]In the case of $3+1$ "fits" [cf. Eqs. (3.2) and (3.3)], we kept the active neutrino parameters fixed at their best-fit values.

strained within their physical limits of 0–2π, and the lightest active neutrino mass eigenvalue m_l to vary unconstrained between 0–0.5 eV. The quotation marks around "fit" and "data" are meant to indicate that our methods are crude, in the sense that we are fitting to previously processed experimental data, assuming a diagonal correlation matrix with Gaussian uncertainties. In order to avoid the subtleties involved in such a "fit to a fit," we hesitate to mention actual confidence intervals but are compelled to do so for lack of a better measure of an allowed region. We sometimes present our best-fit parameter points along with confidence intervals, but we warn the reader to avoid strict interpretations of these numbers. While crude, our methodology of error analysis and fitting provides a very useful instrument for identifying whether (and how) the low-energy seesaw can accommodate a particular combination of data sets.

Before proceeding, it is useful to cement our notation. The neutrino masses will be ordered in ascending order of magnitude from m_1 to m_6 in the case of a normal active neutrino mass hierarchy ($m_2^2 - m_1^2 < m_3^2 - m_1^2$), while in the case of an inverted mass hierarchy they are ordered $m_3 < m_1 < m_2 < m_4 < m_5 < m_6$ (in this case $|m_3^2 - m_1^2| > m_2^2 - m_1^2$). The states with masses $m_{1,2,3}$ are mostly active, while those with masses $m_{4,5,6}$ are mostly sterile. Elements of the mixing matrix are referred to as $U_{\alpha i}$, where $\alpha = e,\ \mu,\ \tau,\ s_1,\ s_2,\ s_3$ (s's are the right-handed neutrino degrees of freedom) and $i = 1, 2, 3, 4, 5, 6$. We also define $\Delta m_{ji}^2 = m_j^2 - m_i^2$ and will refer to the lightest active neutrino mass as m_l. In the case of normal (inverted) active neutrino mass hierarchy $m_l = m_1$ ($m_l = m_3$).

A. Short-baseline oscillation constraints

Here we analyze the constraints imposed on the unknown mixing parameters by current neutrino oscillation data. We will assume that all solar, reactor, long-baseline and atmospheric data are properly fit with active-active oscillations, and that constraints on the other seesaw parameters will be provided mostly by short-baseline accelerator experiments. It is interesting to note that the inclusion of the angles ϕ_{ij} introduces enormous freedom into the system. Any one active-sterile mixing angle contained in Θ can always be set to zero by an appropriate choice of O. In fact, all but three elements may be set to zero simultaneously, with only a single nonzero element in each row and column. In this case, these are constrained to be around $\sqrt{m_l/M_{Ri}}$ where i is the column of the nonzero element. This is especially true when the mostly active neutrino masses are quasidegenerate. An important "sum rule of thumb" is the following. For a given right-handed neutrino mass M_i, the active-sterile mixing angle squared is of order m/M_i, where m is a typical active neutrino mass. One can always choose parameters so that for at most two values of $\alpha = e,\ \mu,\ \tau$, $U_{\alpha i}$ are abnormally small. In that case, however, the "other" $U_{\alpha i}$ is constrained to saturate the bound $|U_{\alpha i}|^2 \lesssim m_l/M_i$.

The most compelling evidence for light sterile neutrinos comes from the short-baseline oscillation experiment by the liquid scintillator neutrino detector (LSND) collaboration at Los Alamos. Using a $\sim$30 MeV $\bar{\nu}_\mu$ beam they observed a better than 3σ excess of $\bar{\nu}_e$-like events above their expected background at their detector some 30 m away from the production point [4]. This evidence of $\bar{\nu}_\mu \leftrightarrow \bar{\nu}_e$ oscillation requires a mass-squared difference greater than $1\,\mathrm{eV}^2$, clearly incompatible with the small mass-squared differences observed between the active neutrinos. Several mechanisms, such as CPT violation [12,16], Lorentz invariance violation [17], quantum decoherence [18], sterile neutrino decay [19] and, of course, oscillation into sterile neutrinos have been proposed to explain this result. Here we concentrate on the last possibility.

In order to take into account all short-baseline data we "fit" our mixing parameters and masses to the results of the $3 + 2$ performed in [15], which are summarized in Table I [20]. Here we assume that the heaviest, mostly sterile state does not participate effectively in LSND oscillations. This is guaranteed to happen if $m_6 \gtrsim 10$ eV. On the other hand, $|U_{\alpha 6}|^2$ are partially constrained by our attempts to accommodate LSND data with seesaw sterile neutrinos, as will become clear in the next subsections.

We find that m_l, the lightest neutrino mass, is constrained to lie between (0.22–0.37) eV, with a "best-fit" value of 0.29 eV. Thus the active neutrino mass spectrum is predicted to be quasidegenerate. A sample 6×6 neutrino mixing matrix that fits all data is

$$U_{3+2} = \begin{pmatrix} 0.8301 & 0.5571 & 0.001\,365 & 0.1193 & -0.009\,399 & -0.006\,513 \\ -0.3946 & 0.5866 & 0.7072 & 0.2016 & 0.2262 & 0.000\,336\,3 \\ 0.3932 & -0.5879 & 0.7070 & 0.4760 & -0.0949 & 0.001\,470 \\ -0.2067 & 0.095\,14 & -0.4792 & 1 & 0 & 0 \\ 0.1343 & -0.1832 & -0.092\,84 & 0 & 1 & 0 \\ 0.004\,963 & 0.004\,295 & -0.001\,268 & 0 & 0 & 1 \end{pmatrix}, \tag{3.1}$$

while the associated masses are $m_1 \simeq m_2 \simeq m_3 = 0.28$ eV, $m_4 = 1.0$ eV, $m_5 = 4.7$ eV, and $m_6 = 6.4$ keV. Note that the matrix in Eq. (3.1) is only approximately unitary, up to corrections of order 25%. This result agrees qualitative with those obtained in [3]. The neutrino masses and mixings obtained in this "fit" are depicted in Fig. 1. We will use the results of "fits" similar to this one throughout the paper.

TABLE I. Parameter values used in our analysis. These were extracted from a fit to all short-baseline neutrino oscillation experiments including LSND within the 3 + 2 scenario [15,20]. 1σ indicates a rough estimate of the 1 sigma allowed range for the different parameters.

	U_{e4}	$U_{\mu 4}$	U_{e5}	$U_{e\mu 5}$	Δm^2_{41} (eV^2)	Δm^2_{51} (eV^2)
Central value	0.121	0.204	0.036	0.224	0.92	22
1σ	0.015	0.027	0.034	0.018	0.08	2.4

One can also aim at a (currently disfavored) 3 + 1 LSND fit.[5] In this case, much lower m_l values are also allowed, extending well into the hierarchical spectrum range. In this case, all m_l values above 0.01 eV and 0.03 eV are allowed, assuming an inverted and normal mass hierarchy, respectively. This is to be compared with the results found in [3], where only trivial choices for O were considered. Examples that "fit" all oscillation data include, for an inverted active mass hierarchy: $m_1 \simeq m_2 = 0.066$ eV, $m_3 = 0.043$ eV, $m_4 = 0.96$ eV, $m_5 = 5$ keV, and $m_6 = 10$ GeV, together with

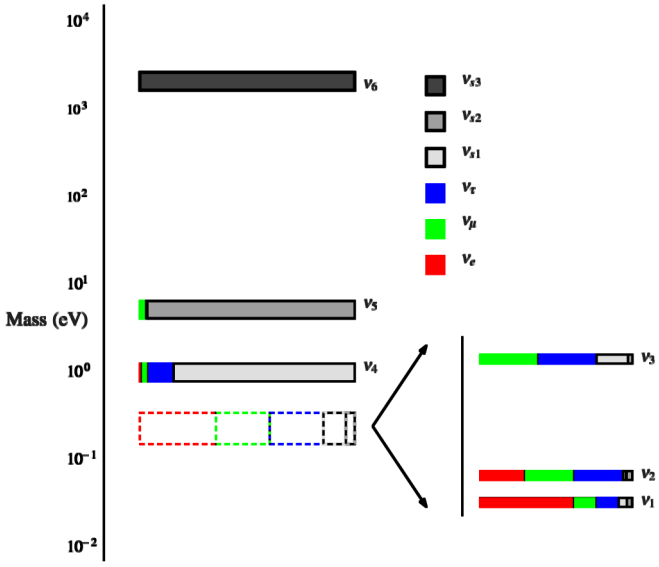

FIG. 1 (color online). Neutrino mass eigenstate spectrum, along with the flavor composition of each state. This case accommodates all neutrino oscillation data, constraints from r-process nucleosynthesis in supernovae, and may help explain anomalous pulsar kicks (see text for details). While we choose to depict a normal hierarchy for the active neutrino states, an inverted active neutrino mass hierarchy would have yielded exactly the same physics (as far as the observables considered are concerned).

$$U_{3+1}^{\text{inverted}} = \begin{pmatrix} 0.8305 & 0.5571 & 0 & 0.1359 & -0.000\,091\,42 & -0.000\,002\,198 \\ -0.3939 & 0.5872 & 0.7071 & 0.2046 & 0.000\,050\,00 & 0.000\,001\,202 \\ 0.3939 & -0.5872 & 0.7071 & -0.044\,21 & -0.003\,236 & -0.000\,000\,185\,7 \\ -0.014\,86 & -0.2218 & -0.1134 & 1 & 0 & 0 \\ 0.001\,370 & -0.001\,878 & 0.002\,253 & 0 & 1 & 0 \\ 0.000\,002\,372 & 0.000\,000\,409\,4 & -0.000\,000\,718\,7 & 0 & 0 & 1 \end{pmatrix}. \tag{3.2}$$

For a normal mass hierarchy, we find that $m_1 = 0.055$ eV, $m_2 = 0.056$ eV, $m_3 = 0.0744$ eV, $m_4 = 0.96$ eV, $m_5 = 5$ keV, $m_6 = 10$ GeV, and

$$U_{3+1}^{\text{normal}} = \begin{pmatrix} 0.8305 & 0.5571 & 0 & 0.1173 & -0.002\,100 & 0.000\,001\,418 \\ -0.3939 & 0.5872 & 0.7071 & 0.2176 & 0.000\,462\,5 & -0.000\,001\,364 \\ 0.3939 & -0.5872 & 0.7071 & 0.098\,02 & 0.002\,804 & 0.000\,001\,283 \\ -0.050\,28 & -0.1355 & -0.2231 & 1 & 0 & 0 \\ 0.000\,821\,4 & 0.002\,545 & -0.002\,310 & 0 & 1 & 0 \\ -0.000\,002\,220 & 0.000\,000\,764\,6 & 0.000\,000\,056\,63 & 0 & 0 & 1 \end{pmatrix}, \tag{3.3}$$

"fit" all oscillation data quite well.

Note that a null result from MiniBooNE is bound to place significant limits on the seesaw energy scale. If all right-handed neutrino masses are similar, the effective mixing angle that governs $\nu_\mu \to \nu_e$ transitions is $\sin^2 2\theta_{\text{MiniBooNE}} \lesssim 4m^2/M^2$. Hence, a null result at MiniBooNE would rule out a seesaw energy scale M lighter than 6 eV, assuming all active neutrino masses m are around 0.1 eV [5]. This limit is sensitive to the lightest neutrino mass m_l and can be somewhat relaxed (similar to how we obtain a good 3 + 2 to all neutrino data) by postulating a (mild) hierarchy of right-handed neutrino masses and by assuming that sterile-electron and sterile-muon neutrino mixing is suppressed with respect to naïve expectations for the lightest mostly sterile state(s). For larger values of m_l, M values around 10 eV are already constrained by $\nu_\mu \to \nu_e$ searches at the NuTeV [21] and

[5]This is easily accomplished by requiring $m_5 \gtrsim 10$ eV.

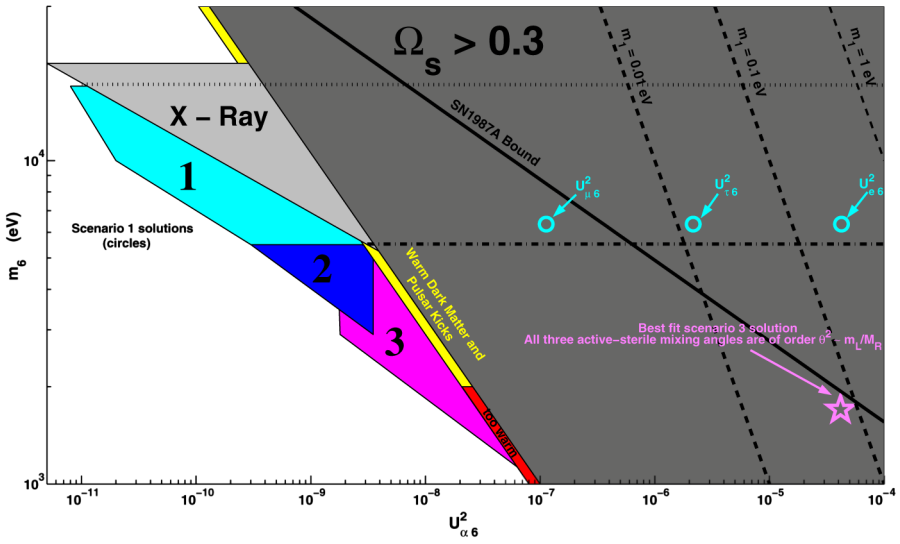

FIG. 2 (color online). Adapted from [51]. Cosmological and astrophysical constraints on the $|U_{\alpha 6}|^2 \times m_6$ plane. In the large dark gray region, the density of a thermal ν_6 population is $\Omega_s > 0.3$, while the light gray "x ray" region is disfavored by x-ray observations. The regions labeled 1,2,3 are preferred if one is to explain anomalous pulsar kicks with active-sterile oscillations inside supernovae. Regions 1 and 3 qualitatively extend inside the $\Omega_s > 0.3$ part of the plane as indicated by the horizontal dotted and dashed-dotted lines, respectively. The regions "warm dark matter" and "too warm dark matter" are meant to represent the region of parameter space where thermal ν_6 qualifies as a good (or bad) warm dark matter candidate. The region above the solid diagonal line is disfavored by the observation of electron (anti)neutrinos from SN1987A. The diagonal dashed lines correspond to $U^2_{e6} = m_l/m_6$, for different values of m_l. Also shown is our "best-fit" sterile solution for different pulsar kick scenarios, assuming the 3 + 2 LSND fit for the lighter states. The regions one and three best-fit values are represented by circles and a star, respectively. See text for details.

NOMAD [22] experiments, and $\nu_\mu \to \nu_\tau$ searches at CHORUS [23].

B. Cosmological and astrophysical constraints, warm dark matter

Very light sterile neutrinos that mix with the active neutrinos are constrained by several cosmological and astrophysical observables. The seesaw right-handed neutrinos are no exception. Given that active-sterile mixing angles $|U_{\alpha i}|^2 \lesssim m_l/m_i$ ($\alpha = e, \mu, \tau$, $i = 4, 5, 6$), it turns out that for "standard cosmology," the right-handed neutrinos thermalize with the early universe thermal bath of SM particles, as long as the reheat temperature is higher than their Majorana masses. For the low seesaw energy scales we are interested in, this is a problem. For the values of M_R under consideration here, thermal right-handed neutrinos easily overclose the Universe. Smaller m_l values ($m_l \lesssim 10^{-5}$ eV) lead to the possibility that right-handed neutrinos are the dark matter, as recently discussed in the literature [7,8]. We comment on this and other possibilities shortly.

Figure 2 depicts the region of the $|U_{e6}|^2 \times m_6$ plane in which the contribution of the heaviest neutrino ν_6 to Ω (the normalized energy density of the Universe, ρ/ρ_c) is larger than 0.3 (dark region). The same constraint roughly applies for all $\alpha = e, \mu, \tau$, and $i = 4, 5, 6$. The dashed diagonal lines correspond to $|U_{\alpha 6}|^2 = m_l/m_6$, for different values of m_l. All lines lie deep within the dark $\Omega_s > 0.3$ region.

For smaller values of M_R, the situation is also constrained. For M_R values below tens of eV, thermal sterile neutrinos contribute to the amount of hot dark matter in the Universe [24–28]. Right-handed neutrinos will thermalize as long as $m_i \sin^2\theta_{i\alpha} \gtrsim 5 \times 10^{-4}$ eV [29,30]. In low-energy seesaws, this roughly translates into $m \gtrsim 10^{-3}$ eV, where m is the active neutrino mass scale. For the cases of interest here $m \gtrsim \sqrt{\Delta m^2_{21}} \sim 10^{-2}$ eV, in which case m_i values above somewhere between[6] 0.2–2 eV are ruled out [24–28,31]. We emphasize, however, that all sterile neutrino solutions to the LSND anomaly face a similar problem, which must be resolved with nonstandard cosmology. We review some possible solutions below. Note that in our "best-fit" 3 + 2 solution to the LSND data, the sum of all active neutrino masses is 0.87 eV, which violates some of the constraints discussed in the literature. This problem can be alleviated if we choose m_l values close to the lower end of the "allowed region," which requires the sum of all active neutrino masses to lie between 0.6 eV and 1 eV. As a concrete example, 0.6 eV is consistent with constraints obtained in [24,26,27]. "Mild"

[6]The upper bound on the sum of neutrino masses from cosmology depends on several assumptions that go into analyzing the different cosmological observations. These include the issue of defining the values of the parameters of the concordance cosmological model and deciding which data sets to include in the fit.

nonstandard cosmology effects (see, for example, [32]) are known to alleviate the hot dark matter bounds on sum of active neutrino masses.

Big-bang nucleosynthesis also proves to be a large obstacle when it comes to the existence of light sterile neutrinos in thermal equilibrium in the early universe (at temperatures above several MeV). In the absence of ''nonstandard'' assumptions, big-bang nucleosynthesis constrains the existence of new thermal relativistic degrees of freedom (see, for example, [28,33]).

One way to avoid the bounds described above (see also, for example, [34]) is to consider that the reheating temperature T_r of the Universe is very low. This way, right-handed neutrinos, in spite of their ''large'' mixing angles, never reach thermal equilibrium in the early universe and neither overclose the Universe nor contribute to the amount of hot dark matter. Quantitatively, $T_r \lesssim 5$ MeV is sufficient to avoid eV-mass (or heavier) sterile neutrinos that are allowed to explain the LSND anomaly [35]. Unless otherwise noted, this is the assumption we make here. Other possibilities include adding new neutrino interactions to lighter scalars, so that neutrinos remain in thermal equilibrium until they are nonrelativistic [32]. According to [32], this can even be accomplished for light neutrinos, as long as the neutrino-scalar field coupling is finely tuned (see, however, [28]). Yet another possibility is to consider that the lepton asymmetry of the Universe is large. The authors of [36] have recently studied this issue in detail and concluded that a lepton asymmetry of order 10^{-4} is required in order to allow the existence of LSND sterile neutrinos to be in agreement with data from large-scale structure and big-bang nucleosynthesis (see also [34]).

Under these circumstances, it is interesting to consider whether light seesaw right-handed neutrinos still qualify as good warm dark matter. This could happen if their production in the early universe was nonthermal. One concern surrounding warm dark matter is whether it is ruled out by large-scale structure surveys. Here, we will not add to this discussion but refer readers to the recent literature on the subject [37]. A brief summary of the situation is as follows: constraints on warm dark matter can be translated into a lower bound on the mostly sterile neutrino mass. The lower bound has been computed by different groups, and lies somewhere between 3 and 14 keV [37]. Different lower bounds depend on several issues, including which subset of Lyman alpha-forest data is taken into account.

Another constraint on potential dark matter sterile neutrinos comes from the observation of x rays originating in galactic clusters. Such regions of the Universe should be overdense with warm dark matter heavy neutrinos, which can be directly observed via their radiative decay $\nu_6 \rightarrow \nu_i + \gamma$ [38]. Bounds from x-ray observations have been summarized very recently in [39]. Combining the results of [39] and Fig. 2, we find that for lightest neutrino masses larger than 10^{-2} eV, such bounds can only be avoided for $m_i \lesssim 100$ eV, where large-scale structure constraints on warm/hot dark matter are severe. This qualitative analysis indicates that seesaw sterile neutrinos cannot, simultaneously, fit the LSND data and serve as cold dark matter.

On the astrophysics side, the most severe constraint on light, sterile neutrinos is provided by the observation of electron (anti)neutrinos coming from SN1987A. The current analysis consists of comparing the model-dependent neutrino flux at the surface of the neutrinosphere with that detected on Earth. Large sterile neutrino mixing and mass would result in modification/depletion of the detected neutrino signal (for a recent detailed discussion, see [40]). Although only 20 neutrinos were observed in this event, one can still place bounds on sterile-active neutrino mixing. As far as ''LSND'' sterile neutrinos are concerned, these bounds are still weaker than those obtained by the null short-baseline oscillation experiments [41] and therefore already accounted for in our analysis. Heavier right-handed neutrinos can, however, be excluded by SN1987A neutrino data. Figure 2 depicts the region of parameter space excluded by SN1987A data (region to the right of solid, diagonal line). This bound is defined by $m_i\sqrt{2}\sqrt{U_{\alpha i}} > 0.22$ keV [35,42]. See also [30]. According to Fig. 2, supernova bounds force the seesaw scale to be below a few keV for m_l values above 0.01 eV.

C. Pulsar kicks

Pulsars are born from the gravitational collapse of the iron core of a massive star. These core collapse supernova are an excellent source of neutrinos, producing all (active) flavors copiously (see [43] for a detailed review). Current observations point to the fact that some pulsars move with peculiar velocities much greater than those expected from an asymmetric supernova explosion mechanism. Quantitatively, current three dimensional models yield velocities up to 200 km/s [44] while pulsars moving at speeds as high as 1600 km/s have been observed. We note, however, that some two-dimensional hydrodynamic studies [45] indicate that natural anisotropies generated during supernova explosions can, in fact, yield large neutron star velocities consistent with observations. More simulations seem to be required in order to validate this claim. Here, we will operate under the hypothesis that new physics, in the form of new neutrino physics, is responsible for the large pulsar kicks.

Since roughly 99% of the approximately 10^{53} ergs of energy released in a core collapse supernova is in the form of neutrinos, it is reasonable that neutrino physics provides a solution to this anomaly. At these rates a small (1–3)% asymmetry in neutrino emission can account for the observed large pulsar velocities. Neutrinos are always *produced* asymmetrically in the polarized medium of the proto-neutron star, due to the left-handed nature of their interactions. Unfortunately, asymmetric production cannot solve this problem because the associated medium den-

sities are such that neutrinos undergo multiple scattering within the star's interior, eventually diffusing out of an effective surface, called the neutrinosphere, with all initial asymmetries washed away. Several distinct mechanisms have been formulated to sidestep this fact. Specifically, the existence of large neutrino magnetic moments has been explored in [46] and can be tested in next generation neutrino scattering experiments [47–49]. Proposed solutions also exist which utilize standard three flavor neutrino oscillations, where ν_μ and ν_τ appearing between their neutrinosphere and the larger ν_e neutrinosphere can stream unhindered out of the star [50]. This solution is, however, currently disfavored by terrestrial oscillation experiments.

We concentrate on the case of oscillations into sterile neutrinos, which can proceed in various ways, depending on the mass and coupling of the relevant neutrinos as well as the properties of the collapsing star, including its density and magnetic field. Following [51], we separate and analyze these within three distinct categories. Each one requires the existence of a keV-scale sterile neutrino with very small couplings to the active flavors, of the order 10^{-4}–10^{-5}, especially if light sterile neutrinos are thermally produced in the early universe. Under these circumstances, if seesaw neutrinos are to play the role of the sterile neutrinos responsible for pulsar kicks, $|U_{\alpha i}|^2 \lesssim m/m_i$ $(i = 4, 5, 6)$ must lie in the 10^{-9} range for $m_i \sim 10^4$ eV. This implies $m \sim 10^{-5}$ eV and is only compatible with a hierarchical active neutrino mass spectrum and very light m_l, as identified in [7,8].

Here, instead, we will concentrate on identifying solutions that will address pulsar kicks and the LSND anomaly. According to the discussion in the previous subsection, the mostly sterile neutrino masses m_4 and m_5 are constrained to be less than 10 eV so that a 3 + 2 solution to the LSND anomaly can be obtained from the seesaw Lagrangian. The heaviest neutrino mass m_6 is unconstrained, so we are free to vary it as needed in order to attack the pulsar peculiar velocity issue.[7] Naïvely, the fraction of ν_α $(\alpha = e, \mu, \tau)$ in ν_6 is expected to be of the order $U_{\alpha 6} \sim \sqrt{0.3 \text{ eV}/3 \times 10^3 \text{ eV}} = 10^{-2}$, much too large to satisfy the pulsar kick plus cosmology constraints summarized in Fig. 2. On the other hand, once the $\Omega_S < 0.3$ constraint is removed, the "pulsar kicks" allowed region of the plane is significantly enlarged, as qualitatively indicated by the horizontal lines in Fig. 2. In this case, which we must consider anyway if we are to have agreement between LSND and the amount of dark matter in the Universe, one can envision explaining pulsar kicks and the LSND data simultaneously. Note that once heavy sterile neutrinos are "removed" (so that they do not overclose the Universe), constraints from x-ray observations (see Fig. 2) are also removed.

[7]We can neglect the lighter sterile neutrinos (ν_4 and ν_5) as they should not alter the kicking mechanism significantly due to their small mass and nonresonant production.

In scenario 1, the pulsar kick is produced via an active-sterile MSW (Mikheyev-Smirnov-Wolfenstein) resonance in the core of the proto-neutron star at large densities, greater than 10^{14} g/cm^3, and magnetic fields, near 10^{16} G [52]. The effective neutrino matter potential in material polarized by a strong magnetic field contains a term proportional to $\vec{k} \cdot \vec{B}/|\vec{k}|$ [53,54], where $\vec{k}$ is the neutrino's three-momentum and $\vec{B}$ is the local magnetic field vector. Clearly, the MSW resonance occurs at a radius that depends on $\vec{k} \cdot \vec{B}/|\vec{k}|$, the relative orientation of the neutrino momentum and magnetic field. Sterile neutrinos produced at smaller radii (higher temperatures) carry greater average momentum than those produced at larger radii (lower temperatures), yielding an asymmetric momentum distribution of emitted neutrinos. This asymmetry is capable of producing the observed pulsar kicks, in the direction of the magnetic field, when the mass and coupling of the sterile state is near 8 keV and above 1.5×10^{-5}, respectively [51]. We found the "best fit" to the LSND data (using ν_4 and ν_5) and pulsar kicks (using ν_6) and $m_6 > 5$ keV. The $|U_{\alpha 6}|^2$ and m_6 "best-fit" values are depicted in Fig. 2. This solution is strongly disfavored by the observation of neutrinos from SN1987A. The fact that $|U_{e6}|$ is much larger than the other two active-sterile mixing angles is due to the fact that $|U_{e4}|$ and $|U_{e5}|$ are constrained by LSND data to be much smaller than naïve expectations [see Eq. (3.1)]. In order to reduce $|U_{e6}|$, one would have to either reduce m_l by an order of magnitude—which renders the 3 + 2 fit to oscillation data very poor—or increase m_6, which would only push $|U_{e6}|$ deeper into the region of parameter space ruled out by SN1987A. One can, however, find 3 + 1 solutions to LSND data where ν_5 could pose as the sterile neutrino that explains why pulsar peculiar velocities are so large [see Eqs. (3.2) and (3.3)].

Scenario 2 also relies on a direction-dependent MSW resonance, this time occurring outside the core where the matter density and temperature are much lower. Here, both the active and sterile neutrinos are free to stream out of the star. The departing active flavors still have a small interaction cross section, $\sigma \sim G_F^2 E_\nu^2$, and can therefore deposit energy and momentum into the star's gravitationally bound envelope proportional to the matter it transverses. Via the direction-dependent resonance, neutrinos moving in the direction of the magnetic field remain active longer, deposit more momentum, and thus kick the star forward. The observations can be explained in this case with a smaller sterile neutrino mass and larger active-sterile coupling near 4 keV and 4.5×10^{-5}, respectively [51]. In the case of our LSND "fit" to the data, we can constrain one of $|U_{\mu 6}|^2$ or $|U_{\tau 6}|^2$ to lie inside region 2. The other $|U_{\alpha 6}|^2$ ($\alpha = e, \tau$ or e, μ), however, are constrained to be large, thus violating the SN1987A bound in much the same way as the scenario 1 best-fit results. Another possibility is to choose all $|U_{\alpha 6}|^2$ of the same order of magnitude. We do not explicitly consider these points as they reside in the region of

parameter space where regions 2 and 3 overlap, and behave in the same way as the point described below, under scenario 3.

Scenario 3 proceeds through off-resonance production of the sterile neutrino in the proto-neutron star core [55]. The amplitude for sterile neutrino production by a weak process is proportional to $U^m_{\alpha 6}$, the effective mixing angle between the heavy mass eigenstate and the flavor eigenstate. Initially, this quantity is very small due to matter effects in the dense core. The effective potential in the star's interior is quickly driven to zero in the presence of sterile neutrino production by a negative feedback mechanism. If this occurs in a time less than the diffusion time scale for the active neutrinos, approximately (3–10) s, the mixing angle will reach its vacuum value [56]. The sterile neutrinos will then be produced and emitted asymmetrically and thus kick the pulsar to large velocities. Lower limits on the vacuum mass and mixing values are derived by requiring that the off-resonance time scale (inversely proportional to $m_6^4 \sin^2 2\theta_{\alpha 6}$) for the evolution of the matter potential to zero be less than about ten seconds. This places the sterile mass and mixing at approximately 1 keV and above 5×10^{-5}, respectively. Since all three active flavors are present in equal abundances, and all contribute to the effective matter potential, the mixing angle in question is not any particular $U_{\alpha 6}$. Rather it is the angle, θ_6 associated with the projection of ν_6 onto the space spanned by ν_e, ν_μ, and ν_τ, that is $\theta_6^2 \equiv U_{e6}^2 + U_{\mu 6}^2 + U_{\tau 6}^2$. From Eq. (2.6) we see that $\theta_6 = \sqrt{m_l/m_6}$ up to corrections due to the nonunitarity of V and active neutrino mass differences. This is independent of mixing angles and therefore cannot be tuned to be small. Our "best-fit" region-3 solution is depicted in Fig. 2 by a star. It turns out that $U_{\alpha 6}$ have very similar values for $\alpha = e, \mu, \tau$. In order to evade the SN1987A constraint, we were forced to pick m_l values close to the lower bound of our 3 + 2 LSND "fit" ($m_l = 0.22$ eV), so that $|U_{e4}|$, $|U_{\mu 4}|$, and $|U_{\mu 5}|$ are close to the low end of the allowed range in Table I.

D. Supernova nucleosynthesis

Core collapse supernova are believed to produce the observed heavy element ($A \geq 100$) abundance through the r-process, or rapid neutron capture process. Here we briefly review this mechanism (see [57] for a comprehensive review), as well as its facilitation by the addition of active-sterile neutrino oscillations [58]. This scenario begins in the neutrino driven wind; that is, the wind of ejected nucleons driven by neutrinos radiated from the cooling proto-neutron star. The maintenance of equilibrium among neutrons, protons, and electron (anti)neutrinos in neutrino capture processes leads to a neutrino-rich environment. As the wind propagates, it cools enough for all free protons to bind into α particles. In the ideal r-process picture, as the wind cools further these α particles bind into intermediate size seed nuclei which later undergo neutron capture to form the observed heavy r-process elements.

This ideal scenario is dampened by the large number of electron neutrinos present at the stage of α particle formation. These will capture on the free neutrons, converting them to protons, which in turn will fuse to make more α particles. The end result is a very small free neutron to α particle ratio, conditions unfavorable for r-process element formation. This is known as the α effect and must be circumvented to produce the correct distribution of heavy elements. A clear solution to this problem is to reduce the number of electron neutrinos present at this stage, which can be accomplished by resonant $\nu_e \rightarrow \nu_s$ conversion[8] [58].

The sterile neutrino solution to the r-process mechanism is modeled and fit to the data in Ref. [59] including the effects of relevant nuclear physics and additional neutrino oscillations in the star's envelope. The analysis is expanded in [60] with the inclusion of fission cycling of the produced heavy elements. The analysis indicates the need for an eV-scale sterile neutrino with an allowed parameter space much larger than that constrained by LSND. By itself, the requirement of successful r-process in supernovae only weakly constrains the light neutrino mass scale to be greater than 10^{-2} eV and 10^{-3} eV for a 1 eV and 10 eV sterile neutrino, respectively. With regard to the LSND results, it has been demonstrated that the 3 + 1 oscillation scenario fits within this parameter space [60]. Considering that the best-fit mass-squared difference and mixing angles for the fourth mass eigenstate, which makes up most of the lightest sterile neutrino, is very similar between the 3 + 1 and 3 + 2 case [20], it is reasonable to conclude that $\nu_e \leftrightarrow \nu_{s4}$ resonant conversion will also fit within this scenario. Even oscillations into the heavier ν_{s5} state can potentially solve this anomaly if the neutrino driven wind expansion time scale is sufficiently small, ≤ 0.1 sec. To conclude this section we note that, although the sterile neutrino solution to the supernova nucleosynthesis problem fits well within our seesaw framework, it adds no additional constraints and therefore does not increase the predictability of our scenario.

IV. OTHER PROBES OF THE SEESAW ENERGY SCALE

Here we survey other existing and future probes of light sterile neutrinos. As opposed to the previous cases, these probes are perfectly consistent by themselves. That is, extra heavy neutrinos are not required to solve problems

[8] In this mechanism the effective matter potential, which depends on the number of electrons, positrons, and neutrinos, varies wildly as a function of distance from the core. Along this radial direction there are three relevant MSW resonant conversions that must be tracked and understood: $\nu_e \rightarrow \nu_s$, $\bar{\nu}_e \rightarrow \bar{\nu}_s$, and $\bar{\nu}_s \rightarrow \bar{\nu}_e$. See [58] for more information.

within the system. However, their addition can lead to large modifications to the outcome of such experiments, thus rendering the eV-scale seesaw scenario testable. Specifically, we consider bounds from tritium beta decay and neutrinoless double-beta decay. Observations in all of these areas have already yielded useful constraints on sterile neutrinos, and the situation is expected to improve in the next few years.

A. Tritium beta decay

The end point of the electron energy spectrum in the beta decay of tritium is a powerful probe of nonzero neutrino masses. This results from the decay kinematics of the system which is necessarily modified by the presence of a massive neutrino. The nonzero neutrino mass effect can be understood almost entirely from the analysis of the phase space distribution of the emitted electrons and is therefore quite model independent. Existing beta-decay experiments extract limits on an effective electron neutrino mass $m^2_{\nu_e} = \sum_i |U_{ei}|^2 m_i^2$ [61], provided that the neutrino masses are smaller than the detector energy resolution. Currently the most stringent bounds on $m^2_{\nu_e}$ are $(2.3)^2$ eV^2 at 95% confidence from the Mainz experiment [62] and $(2.5)^2$ eV^2 at 95% confidence from the Troitsk experiment [63]. In the next few years the Katrin experiment should exceed these limits by nearly 2 orders of magnitude, probing down to $(0.2)^2$ eV^2 at the 90% confidence level [64]. One might naïvely compute this effective mass for the best-fit mixing parameters obtained in the previous section. In this case, we expect a keV seesaw neutrino to contribute to $m^2_{\nu_e}$ by a huge amount $\delta m^2_{\nu_e} = U^2_{e6} m_6^2 \sim \frac{m_l}{m_6} m_6^2 = m_l m_6$ [3] so that it would be excluded by the current precision measures of tritium beta decay for $m_l \gtrsim 10^{-3}$ eV. This is clearly an incorrect treatment of the physics. As pointed out in, for example, [65], the existence of a heavy neutrino state would produce a kink in the electron energy spectrum of size $|U_{ei}|^2$ at an energy $E_0 - m_i$ as well as a suppression of events at the end point of order $1 - |U_{ei}|^2$. Here U_{ei} $(i = 4, 5, 6)$ is the mixing between the electron neutrino flavor eigenstate and the heavy mass eigenstate, while $E_0 = 18.6$ keV is the end point energy of tritium beta decay.

Figure 3 depicts $1 - S/S_0$, where S is the β-ray energy spectrum obtained assuming three mostly active, degenerate neutrinos with mass $m = 0.1$ eV and one mostly sterile neutrino ν_i with various masses m_i and mixing angle $U^2_{ei} = m/m_i$, while S_0 is the spectrum associated with massless neutrinos. One can readily observe "kinks" in the spectrum above m_i. For β energies above $E_0 - m_i$, the impact of the sterile state is to "remove" around $1 - |U_{ei}|^2$ of the β rays from spectrum. This is most significant between $E_0 - m_i$ and E_0 minus the mass of the active neutrinos. For energies below $E_0 - m_i$, the spectrum agrees with that obtained from the emission of one effective neutrino with mass-squared $m^2_{\nu_e}$.

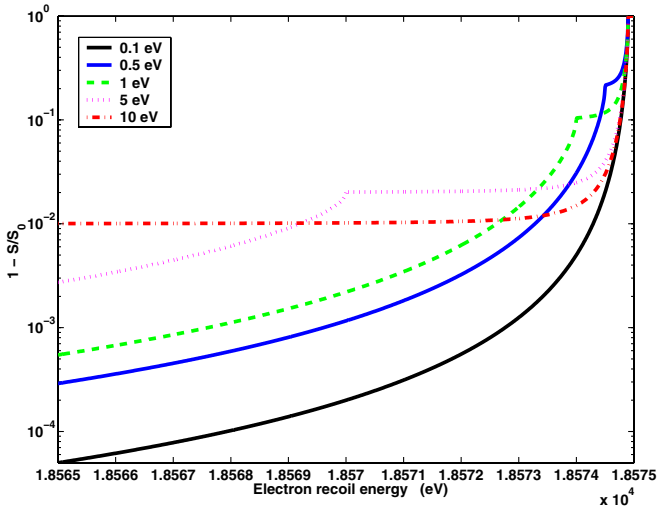

FIG. 3 (color online). $1 - S/S_0$ as a function of the β-ray energy, where S is the β-ray energy spectrum obtained assuming three mostly active, degenerate neutrinos with mass $m = 0.1$ eV and one mostly sterile neutrino ν_i with $m_i = 0.1$, 0.5, 1,5, and 10 eV. The mixing angle is given by $U^2_{ei} = m/m_i$. S_0 is the spectrum associated with massless neutrinos. See text for details.

We estimate the sensitivity of future tritium beta-decay experiments to the emission of one heavy state by considering the ratio between the number of electrons with energies above $E_0 - \Delta E$ in the case of one heavy massive neutrino ν_i and in the case of massless neutrinos

$$R(U_{ei}, M_R) = \left[|U_{ei}|^2 \int_{E_0-\Delta E}^{E_0} dE \frac{dN}{dE}(m_i) + (1 - |U_{ei}|^2) \times \int_{E_0-\Delta E}^{E_0} dE \frac{dN}{dE}(0) \right] \Big/ \int_{E_0-\Delta E}^{E_0} dE \frac{dN}{dE}(0), \tag{4.1}$$

where dN/dE is the energy distribution of β rays, which depends on the neutrino mass m_i. This expression can be easily generalized for more than one heavy neutrino. The advantage of using the ratio above is that potential systematic uncertainties and normalization effects can be safely ignored. An experiment is sensitive to a massive neutrino state if it can distinguish R from unity, a determination that should be limited by statistics due to the very low β-ray flux in the high-energy tail of the electron spectrum.

In order to compute R, we use an analytic expression for Eq. (4.1), which exists provided that one neglects nucleon recoil in the decay. Figure 4 depicts constant R contours in the $|U_{ei}| \times m_i$ plane. Contours were computed for $\Delta E = 25$ eV, in order to allow one to easily compare our results with the sensitivity estimates of the Katrin experiment. After data-taking, Katrin is expected to measure R at the 0.1%–1% level (lightest gray region). Its sensitivity is expected to be $\sqrt{m^2_{\nu_e}} > 0.2$ eV at the 90% confidence level. This can be extracted from the plot by concentrating on the $U_{ei} = 1$ line. Note that while the expected energy resolu-

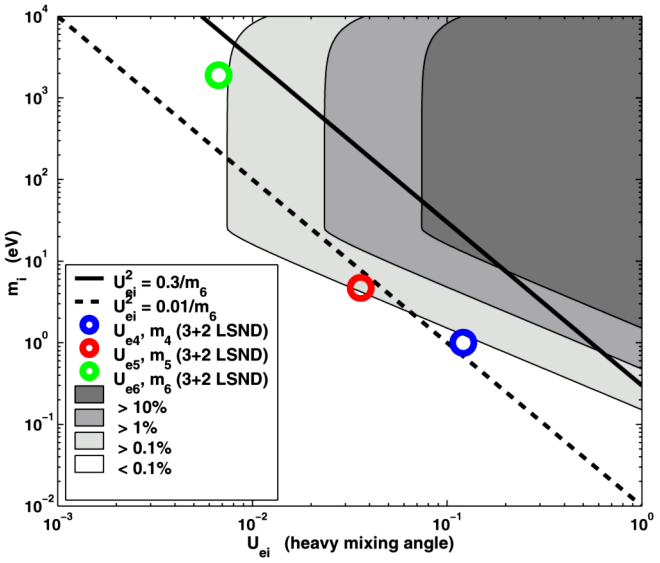

FIG. 4 (color online). Contour plot of constant R, as defined by Eq. (4.1), assuming an energy window $\Delta E = 25$ eV. The solid (dashed) line corresponds to $\sqrt{m_l/m_i}$, a naïve upper bound for $|U_{ei}|$, for $m_l = 0.3$ eV (0.01 eV). The circles correspond to U_{ei} for the three mostly sterile states obtained by our "fit" to other neutrino data, Eq. (3.1). See text for details.

tion for Katrin is of order 1 eV, the expected number of signal events above $E_0 - 1$ eV is minuscule (both in absolute terms and compared with expected number of background events), so that most of the sensitivity to nonzero neutrino masses comes from analyzing the shape of the electron spectrum in the last tens of electron volts. A larger "window" would suffer from increased systematic uncertainties, so that $\Delta E \sim 25$ eV is representative of Katrin's optimal reach [64].

The shape of the constant R contours is easy to understand. As already discussed, for $m_i > \Delta E$, the effect of the right-handed neutrinos is to reduce the spectrum in an energy independent way by $1 - |U_{ei}|^2$, while for $m_i < \Delta E$, states with the same effective mass-squared $m_i^2|U_{ei}|^2$ produce the same effect in tritium beta decay so that the diagonal lines coincide with lines of constant $m_i^2|U_{ei}|^2$.

A more sensitive approach would be to "bin" the last tens of eV of the data into 1 eV bins, and fit the distribution to a massless neutrino hypothesis. For the values of the parameters in which we are interested, we find that one 25 eV bin yields roughly the same sensitivity to nonzero neutrino masses as 25 1 eV bins for large masses and small mixing angles. For smaller masses and larger mixing angles, a "binned" analysis should be sensitive to effects which are localized in individual bins (such as kinks). Another recent estimate of the sensitivity of tritium beta-decay experiments to heavy, sterile neutrinos can be found in [30]. Our results agree qualitatively.

Figure 4 also depicts the loose upper bound for $U_{ei} = \sqrt{m_l/m_i}$ as a function m_i, for $m_l = 0.32$ eV and $m_l = 0.01$ eV. For $m_l \gtrsim 0.1$ eV, Katrin should be sensitive to $M_R \lesssim 1$ keV while for $m_l \gtrsim 0.01$ eV (the solar mass scale) Katrin should be sensitive to $M_R \gtrsim 10$ eV and $M_R \lesssim 100$ eV, where here we assume that all right-handed neutrino masses are of order M_R. In the case of seesaw parameters that fit the LSND data with a $3 + 2$ neutrino spectrum [see Eq. (3.1)], expectations are high as far as observing a kinematical neutrino mass effect at Katrin, in spite of the fact that the fit to LSND data requires U_{e4} and U_{e5} to be "abnormally" low. Figure 4 depicts U_{ei} and m_i values for the heavy neutrinos (open circles). The contribution of the heaviest of the two LSND-related sterile neutrinos is of order the Katrin sensitivity, while the active contribution itself, which leads to $m^2_{\nu_e} = \sum_{i=1,2,3}|U^2_{ei}m^2_i| \sim m^2_l$ is already within the Katrin sensitivity range, given that large $m_l > 0.22$ eV values are required by our $3 + 2$ LSND "fit." The effect of ν_6 is small if m_6 is larger than 1 keV (required if one takes the "pulsar kicks" hint into account), but would be very significant if m_6 were less than 1 keV.

B. Neutrinoless double-beta decay

If the neutrinos are Majorana fermions—as predicted in the case of interest here—lepton number is no longer a conserved quantity. The best experimental probe of lepton-number violation is the rate for neutrinoless double-beta decay. This process, which violates lepton number by two units, is currently the subject of intense search [66]. If neutrino masses are the only source of lepton-number violation, the decay width for neutrinoless double-beta decay is

$$\Gamma_{0\nu\beta\beta} \propto \left| \sum_i U^2_{ei} \frac{m_i}{Q^2 + m_i^2} \mathcal{M}(m_i^2, Q^2) \right|^2, \tag{4.2}$$

where $\mathcal{M}$ is the relevant nuclear matrix element and $Q^2 \sim 50^2$ MeV^2 is the relevant momentum transfer. In the limit of very small neutrino masses ($m_i^2 \ll Q^2$), $\Gamma_{0\nu\beta\beta}$ is proportional to an effective neutrino mass $|m_{ee}|$,

$$m_{ee} = \sum_i^n U^2_{ei} m_i. \tag{4.3}$$

The sum is over all light neutrino mass eigenstates. In the case of a low-energy seesaw, when all m_i, $i = 1, \ldots, 6$ are much smaller than Q^2, it is easy to see that m_{ee} vanishes [3]. The reason for this is that, in the weak basis we are working on (diagonal charged-lepton and charged-weak current), m_{ee} is the ee-element of the neutrino mass matrix, as defined in Eq. (2.2). One can trivially check that, by assumption, not only does m_{ee} vanish, but so do all other $m_{\alpha\beta}$, $\alpha, \beta = e, \mu, \tau$. Note that this result does not depend on the fact that we have been assuming all elements of the neutrino mass matrix to be real [67].

For heavy ν_i neutrinos, $U^2_{ei}m_i$ no longer captures the dependency of $\Gamma_{0\nu\beta\beta}$ on the exchange of ν_i. For $m_i^2 \gg Q^2$,

instead, the dependency on neutrino exchange is proportional to U_{ei}^2/m_i. If this is the case, the overall contribution (including all heavy and light states) is no longer proportional to m_{ee} but, instead, can be qualitatively expressed as a function of an effective $m_{ee}^{\rm eff}$,

$$m_{ee}^{\rm eff} \equiv Q^2 \sum_i \frac{U_{ei}^2 m_i}{Q^2 + m_i^2}. \tag{4.4}$$

The approximation $\Gamma_{0\nu\beta\beta} \propto |m_{ee}^{\rm eff}|$ is good as long as one can neglect the dependency of $\mathcal{M}$ on m_i and is not expected to be a great approximation when $m_i^2 \sim Q^2$. Nonetheless, $m_{ee}^{\rm eff}$ still qualitatively captures the behavior of $\Gamma_{0\nu\beta\beta}$ as a function of the sterile neutrino masses and studying its behavior is sufficient for our ambitions in this discussion.

Figure 5 depicts $m_{ee}^{\rm eff}$ for our "best-fit" 3 + 2 LSND solution (see Sec. III A), as a function of the unconstrained m_6. As advertised, $m_{ee}^{\rm eff}$ vanishes for $m_6^2 \ll Q^2$. The figure also depicts the "active only" value of $m_{ee}^{\rm active} = \sum_{i=1,2,3} U_{ei}^2 m_i$. Even in the limit $m_6^2 \gg Q^2$, there is still partial cancellation between the mostly active and mostly sterile LSND states. This is a feature of the Lagrangian we are exploring here, and is not in general observed in other scenarios with light sterile neutrinos tailor-made to solve the LSND anomaly.

Currently, the most stringent limits on this effective mass comes from the Heidelberg-Moscow experiment [68] where they find $m_{ee} < 0.91$ eV at 99% confidence. In the near future, experiments aim to reach down to m_{ee} values close to 10^{-2} eV [66]. A signal would rule out a seesaw scale below tens of MeV. On the other hand, if we were to conclude that the neutrino masses are quasidegenerate (through, say, a signal in tritium beta decay) and if the LSND 3 + 2 solution were experimentally confirmed, a vanishing result for m_{ee} could be considered strong evidence for a very small seesaw scale. On the other hand, if this were the case (m_{ee} zero, large active neutrino masses), it would also be very reasonable to conclude that neutrinos are Dirac fermions. Distinguishing between the two possibilities would prove very challenging indeed. It is curious (but unfortunate) that in a low-energy seesaw model the neutrinos are Majorana fermions, but all "standard" lepton-number violating observables vanish, given that their rates are all effectively proportional to $m_{\alpha\beta}$.

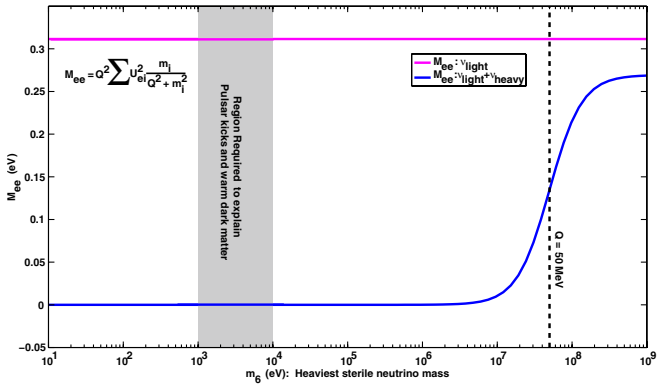

FIG. 5 (color online). Effective m_{ee} for neutrinoless double-beta decay as a function of m_6, the heaviest right-handed neutrino mass, assuming the existence of only light, active, neutrinos (magenta curve), with a degenerate mass spectra, and for our "best-fit" 3 + 2 LSND sterile neutrino solution (blue curve). See text for details. Also indicated is the parameter region preferred by astrophysical hints of sterile neutrinos. We assume $Q = 50$ MeV. In the case of a low-energy seesaw, m_{ee} vanishes as long as $m_6 \ll Q$.

V. CONCLUDING REMARKS

The "new standard model" (equal to the "old" standard model plus the addition of three gauge-singlet Weyl fermions) is, arguably, the simplest extension of the SM capable of accommodating neutrino masses. This Lagrangian contains a new dimension-full parameter: the right-handed neutrino mass scale M, which must be determined experimentally. Unlike the Higgs mass-squared parameter, all M values are technically natural given that the global symmetry of the Lagrangian is enhanced in the limit $M \to 0$.

Very large M values are *theoretically* very intriguing and have received most of the attention of the particle physics community. There are several strong hints that new phenomena are expected at the electroweak breaking scale $\sim 10^3$ GeV, the grand unified scale $\sim 10^{15-16}$ GeV, and the Planck scale $\sim 10^{18-19}$ GeV, and it is tempting to associate M to one of these energy scales. Furthermore, large M values provide an elegant mechanism for generating the matter antimatter asymmetry of the Universe [69]. Of course, large M values are experimentally very frustrating. It may ultimately prove impossible to experimentally verify whether the new standard model is really the correct way to describe nature.

Here, we explore the opposite end of the M spectrum, $M \lesssim 1$ keV. Such values are *phenomenologically* very intriguing, given that small M values imply the existence of light sterile neutrinos that mix significantly with the active neutrinos and can potentially be directly observed. Furthermore, there are several experimental and astrophysical phenomena that are best understood if one postulates the existence of light, moderately mixed sterile neutrinos. We find that by requiring all three right-handed neutrino masses to be less than a few keV we can simultaneously explain all neutrino oscillation data, including those from LSND, explain the large peculiar velocities of pulsars, and accommodate the production of heavy elements in supernova environments. Our fit also provides constraints for the active neutrino oscillation parameters, most strongly to the lightest active neutrino mass. All successful parameter choices that accommodate the LSND data require m_l to be large ($m_l \gtrsim 0.1$ eV), and the "best fit" requires all

active neutrino masses to be quasidegenerate. It is important to emphasize that the presence of light sterile neutrinos that mix relatively strongly with the active neutrinos is only in agreement with cosmological data (especially large-scale structure and big-bang nucleosynthesis) if nonstandard cosmological ingredients are present.

Figure 1 depicts such a scenario. This six neutrino mass spectrum (including mixing angles) fits all neutrino oscillation data (including those from LSND), provides a sterile neutrino solution to the pulsar kick puzzle, and contains all the necessary ingredients for heavy element nucleosynthesis in supernovae. The heaviest of the neutrinos does not qualify as thermal warm dark matter (in the absence of new cosmological ingredients, its presence would overclose the Universe). Note that even if it were nonthermally produced, constraints from the observation of x rays from the center of the galaxy would rule out ν_6 as a good dark matter candidate. Lighter ν_6 masses will evade x-ray constraints but would render ν_6 too ''hot,'' and hence a poor dark matter candidate.

On the negative side, low M values are, theoretically, rather puzzling. In order to obtain the observed light neutrino masses, neutrino Yukawa couplings are required to be much smaller than the electron Yukawa coupling, and it is tempting to believe that such small numbers are proof that a more satisfying understanding of fermion masses must exist. Furthermore, thermal leptogenesis is no longer an option (see, however, [70]). Finally, the fact that M is naïvely unrelated to other mass scales can also be perceived as disheartening, but, in our opinion, should be interpreted as evidence that there is more to the lepton sector than meets the eye.

Regardless of one's preference for a high or low seesaw energy scale, and independent of whether the data from LSND and the astronomical observables discussed above have anything to do with sterile neutrinos, our main point is that the determination of M is an *experimental* issue. In the near/intermediate future, low-energy seesaw scales will be probed by several experiments, most importantly measurements of the end point of tritium beta decay, the MiniBooNE experiment, searches for neutrinoless double-beta decay and, if we get lucky, the detection of neutrinos from a nearby supernova explosion. We find, for example, that Katrin should be sensitive to seesaw energy scales below tens of keV if all right-handed neutrino masses are similar, while null results from MiniBooNE would severely constrain right-handed neutrino masses below several eV. We conclude by pointing out that larger (but still ''small'') values of M are much harder to constrain. For GeV sterile neutrinos, typical active-sterile mixing angles are $U^2_{\alpha i} \lesssim 10^{-10}$, probably too small to observe in particle physics processes. It is frustrating (and, we hope, ultimately false) that we seem to be unable to experimentally distinguish $M \sim 1$ GeV from $M \sim 10^{14}$ GeV...

ACKNOWLEDGMENTS

We thank Irina Mocioiu for comments on how the pulsar kick requirements extend toward the $\Omega_s \> 0.3$ region, Michel Sorel for discussions regarding $3 + 2$ fits to the neutrino oscillation data, and Alex Friedland for comments on large pulsar kicks from standard supernova dynamics. J. J. would also like to thank the students and lecturers of the TASI 2006 summer school for useful discussions of this manuscript and many related physical concepts. This work is sponsored in part by DOE Grant No. DE-FG02-91ER40684.

[1] A. Strumia and F. Vissani, hep-ph/0606054; R. N. Mohapatra and A. Yu. Smirnov, hep-ph/0603118; R. N. Mohapatra *et al.*, hep-ph/0510213; A. de Gouvêa, hep-ph/0411274; Mod. Phys. Lett. A **19**, 2799 (2004).
[2] P. Minkowiski, Phys. Lett. **67B**, 421 (1977); M. Gell-Mann, P. Ramond, and R. Slansky, in *Supergravity*, edited by D. Freedman and P. Van Niuenhuizen (North Holland, Amsterdam, 1979), p. 315; T. Yanagida, in *Proceedings of the Workshop on Unified Theory and Baryon Number in the Universe*, edited by O. Sawada and A. Sugamoto (KEK, Tsukuba, Japan, 1979); S. L. Glashow, *1979 Cargèse Lectures in Physics—Quarks and Leptons*, edited by M. Lévy *et al.* (Plenum, New York, 1980), p. 707; R. N. Mohapatra and G. Senjanović, Phys. Rev. Lett. **44**, 912 (1980).
[3] A. de Gouvêa, Phys. Rev. D **72**, 033005 (2005).
[4] A. Aguilar *et al.* (LSND Collaboration), Phys. Rev. D **64**, 112007 (2001).
[5] A. Bazarko (MiniBooNE Collaboration), Nucl. Phys. B, Proc. Suppl. **91**, 210 (2001).
[6] W. Krolikowski, Acta Phys. Pol. B **35**, 2241 (2004).
[7] T. Asaka, S. Blanchet, and M. Shaposhnikov, Phys. Lett. B **631**, 151 (2005).
[8] T. Asaka, A. Kusenko, and M. Shaposhnikov, Phys. Lett. B **638**, 401 (2006).
[9] J. A. Casas and A. Ibarra, Nucl. Phys. **B618**, 171 (2001).
[10] M. Maltoni, T. Schwetz, M. A. Tortola, and J. W. F. Valle, New J. Phys. **6**, 122 (2004).
[11] W.-M. Yao *et al.* (Particle Data Group), J. Phys. G **33**, 1 (2006).
[12] A. Strumia, Phys. Lett. B **539**, 91 (2002).
[13] M. Maltoni, T. Schwetz, M. A. Tortola, and J. W. F. Valle, Nucl. Phys. **B643**, 321 (2002).
[14] M. Maltoni, T. Schwetz, M. A. Tortola, and J. W. F. Valle, hep-ph/0305312.
[15] M. Sorel, J. M. Conrad, and M. Shaevitz, Phys. Rev. D **70**,

073004 (2004).
[16] H. Murayama and T. Yanagida, Phys. Lett. B **520**, 263 (2001); G. Barenboim, L. Borissov, J. D. Lykken, and A. Yu. Smirnov, J. High Energy Phys. 10 (2002) 001; M. C. Gonzalez-Garcia, M. Maltoni, and T. Schwetz, Phys. Rev. D **68**, 053007 (2003).
[17] V. A. Kostelecky and M. Mewes, Phys. Rev. D **70**, 076002 (2004); **69**, 016005 (2004); L. B. Auerbach *et al.* (LSND Collaboration), Phys. Rev. D **72**, 076004 (2005); A. de Gouvêa and Y. Grossman, Phys. Rev. D **74**, 093008 (2006); T. Katori, A. Kostelecky, and R. Tayloe, Phys. Rev. D **74**, 105009 (2006).
[18] G. Barenboim and N. E. Mavromatos, J. High Energy Phys. 01 (2005) 034.
[19] S. Palomares-Ruiz, S. Pascoli, and T. Schwetz, J. High Energy Phys. 09 (2005) 048.
[20] M. Sorel (private communication).
[21] S. Avvakumov *et al.*, Phys. Rev. Lett. **89**, 011804 (2002).
[22] P. Astier *et al.* (NOMAD Collaboration), Phys. Lett. B **570**, 19 (2003).
[23] E. Eskut *et al.* (CHORUS Collaboration), Phys. Lett. B **434**, 205 (1998); **424**, 202 (1998).
[24] D. N. Spergel *et al.*, astro-ph/0603449.
[25] U. Seljak, A. Slosar, and P. McDonald, J. Cosmol. Astropart. Phys. 10 (2006) 014.
[26] S. Hannestad and G. G. Raffelt, J. Cosmol. Astropart. Phys. 11 (2006) 016.
[27] G. L. Fogli *et al.*, hep-ph/0608060.
[28] M. Cirelli and A. Strumia, astro-ph/0607086.
[29] K. Enqvist, K. Kainulainen, and M. J. Thomson, Nucl. Phys. **B373**, 498 (1992); X. Shi, D. N. Schramm, and B. D. Fields, Phys. Rev. D **48**, 2563 (1993).
[30] A. Yu. Smirnov and R. Z. Funchal, Phys. Rev. D **74**, 013001 (2006).
[31] S. Dodelson, A. Melchiorri, and A. Slosar, Phys. Rev. Lett. **97**, 041301 (2006).
[32] See, for example, J. F. Beacom, N. F. Bell, and S. Dodelson, Phys. Rev. Lett. **93**, 121302 (2004).
[33] See, for example, V. Barger, J. P. Kneller, H. S. Lee, D. Marfatia, and G. Steigman, Phys. Lett. B **566**, 8 (2003).
[34] K. Abazajian, N. F. Bell, G. M. Fuller, and Y. Y. Y. Wong, Phys. Rev. D **72**, 063004 (2005).
[35] G. Gelmini, S. Palomares-Ruiz, and S. Pascoli, Phys. Rev. Lett. **93**, 081302 (2004).
[36] For a recent analysis, see Y. Z. Chu and M. Cirelli, Phys. Rev. D **74**, 085015 (2006).
[37] For very recent discussions, see K. Abazajian, Phys. Rev. D **73**, 063513 (2006); U. Seljak, A. Makarov, P. McDonald, and H. Trac, Phys. Rev. Lett. **97**, 191303 (2006); K. Abazajian and S. M. Koushiappas, Phys. Rev. D **74**, 023527 (2006); M. Viel, J. Lesgourgues, M. G. Haehnelt, S. Matarrese, and A. Riotto, Phys. Rev. Lett. **97**, 071301 (2006).
[38] K. Abazajian, G. M. Fuller, and W. H. Tucker, Astrophys. J. **562**, 593 (2001). Recent discussions can be found in K. Abazajian and S. M. Koushiappas in [37]; C. R. Watson, J. F. Beacom, H. Yuksel, and T. P. Walker, Phys. Rev. D **74**, 033009 (2006).
[39] A. Kusenko, astro-ph/0608096.
[40] M. Cirelli, G. Marandella, A. Strumia, and F. Vissani, Nucl. Phys. **B708**, 215 (2005).
[41] M. Sorel and J. M. Conrad, Phys. Rev. D **66**, 033009 (2002).
[42] K. Kainulainen, J. Maalampi, and J. T. Peltoniemi, Nucl. Phys. **B358**, 435 (1991).
[43] H. A. Bethe, Rev. Mod. Phys. **62**, 801 (1990).
[44] Z. Arzoumanian, D. F. Chernoffs, and J. M. Cordes, Astrophys. J. **568**, 289 (2002).
[45] L. Scheck, T. Plewa, H. T. Janka, K. Kifonidis, and E. Mueller, Phys. Rev. Lett. **92**, 011103 (2004); L. Scheck, K. Kifonidis, H. T. Janka, and E. Mueller, astro-ph/0601302.
[46] M. B. Voloshin, Phys. Lett. B **209**, 360 (1988).
[47] A. de Gouvêa and J. Jenkins, Phys. Rev. D **74**, 033004 (2006).
[48] Z. Daraktchieva *et al.* (MUNU Collaboration), Phys. Lett. B **615**, 153 (2005).
[49] H. B. Li *et al.* (TEXONO Collaboration), Phys. Rev. Lett. **90**, 131802 (2003).
[50] A. Kusenko and G. Segre, Phys. Rev. Lett. **77**, 4872 (1996).
[51] A. Kusenko, Int. J. Mod. Phys. D **13**, 2065 (2004).
[52] M. Barkovich, J. C. D'Olivo, and R. Montemayor, hep-ph/0503113.
[53] H. Nunokawa, V. B. Semikoz, A. Yu. Smirnov, and J. W. F. Valle, Nucl. Phys. **B501**, 17 (1997).
[54] S. Esposito and G. Capone, Z. Phys. C **70**, 55 (1996).
[55] G. M. Fuller, A. Kusenko, I. Mocioiu, and S. Pascoli, Phys. Rev. D **68**, 103002 (2003).
[56] K. Abazajian, G. M. Fuller, and M. Patel, Phys. Rev. D **64**, 023501 (2001).
[57] S. Wanajo, T. Kajino, G. J. Mathews, and K. Otsuki, astro-ph/0102261.
[58] G. C. McLaughlin, J. M. Fetter, A. B. Balantekin, and G. M. Fuller, Phys. Rev. C **59**, 2873 (1999).
[59] J. Fetter, G. C. McLaughlin, A. B. Balantekin, and G. M. Fuller, Astropart. Phys. **18**, 433 (2003).
[60] J. Beun, G. C. McLaughlin, R. Surman, and W. R. Hix, Phys. Rev. D **73**, 093007 (2006).
[61] Y. Farzan and A. Yu. Smirnov, Phys. Lett. B **557**, 224 (2003).
[62] C. Kraus *et al.*, Eur. Phys. J. C **40**, 447 (2005).
[63] V. M. Lobashev *et al.*, Nucl. Phys. B, Proc. Suppl. **91**, 280 (2001).
[64] A. Osipowicz *et al.* (KATRIN Collaboration), hep-ex/0109033.
[65] Y. Farzan, O. L. G. Peres, and A. Yu. Smirnov, Nucl. Phys. **B612**, 59 (2001).
[66] S. R. Elliott and P. Vogel, Annu. Rev. Nucl. Part. Sci. **52**, 115 (2002); F. T. Avignone, Nucl. Phys. B, Proc. Suppl. **143**, 233 (2005).
[67] B. Kayser, Phys. Rev. D **30**, 1023 (1984).
[68] A. M. Bakalyarov, A. Y. Balysh, S. T. Belyaev, V. I. Lebedev, and S. V. Zhukov (C03-06-23.1 Collaboration), Pisma Fiz. Elem. Chast. Atom. Yadra **2**, 21 (2005) [Phys. Part. Nucl. Lett. **2**, 77 (2005)].
[69] For a recent review, see W. Buchmuller, R. D. Peccei, and T. Yanagida, Annu. Rev. Nucl. Part. Sci. **55**, 311 (2005).
[70] M. Shaposhnikov and I. Tkachev, Phys. Lett. B **639**, 414 (2006).